Published in final edited form as:

J Biomech. 2018 May 17; 73: 99–107. doi:10.1016/j.jbiomech.2018.03.040.

Mechanical strain induced phospho-proteomic signaling in uterine smooth muscle cells

Christian Copley Salem[1,4], **Craig Ulrich**[1,4], **David Quilici**[2,3], **Karen Schlauch**[3], **Iain LO Buxton**[1], and **Heather Burkin**[1,5]

[1]University of Nevada, Reno School of Medicine, Department of Pharmacology

[2]University of Nevada, Reno School of Medicine, Mick Hitchcock Proteomics Center

[3]University of Nevada, Reno School of Medicine, Department of Biochemistry

Abstract

Mechanical strain associated with the expanding uterus correlates with increased preterm birth rates. Mechanical signals result in a cascading network of protein phosphorylation events. These signals direct cellular activities and may lead to changes in contractile phenotype and calcium signaling. In this study, the complete phospho-proteome of uterine smooth muscle cells subjected to mechanical strain for 5 min was compared to un-strained controls. Statistically significant, differential phosphorylation events were annotated by Ingenuity Pathway Analysis to elucidate mechanically induced phosphorylation networks. Mechanical strain leads to the direct activation of ERK1/2, HSPB1, MYL9, in addition to phosphorylation of PAK2, vimentin, DOCK1, PPP1R12A, and PTPN11 at previously unannotated sites. These results suggest a novel network reaction to mechanical strain and reveal proteins that participate in the activation of contractile mechanisms leading to preterm labor.

[5]Corresponding Author: Heather Burkin, Ph.D., Department of Pharmacology, Center for Molecular Medicine 307E, Reno, Nevada 89557-0318, Phone: (775) 784-6289, Fax: (775) 784-1620, hburkin@med.unr.edu.
[4]These authors contributed equally to this work

All authors have made contributions as follows:

Christian Copley Salem: Acquisition of data, interpretation of data, drafting the article, and final approval of the submission.

Craig Ulrich: Conception and design, acquisition of data, interpretation of data, drafting the article, and final approval of the submission.

David Quilici: Conception and design, acquisition of data, interpretation of data, drafting the article, and final approval of the submission.

Karen Schlauch: Analysis and interpretation of data, drafting the article, and final approval of the submission.

Iain LO Buxton: Analysis and interpretation of data, drafting the article, and final approval of the submission.

Heather Burkin: Conception and design, acquisition of data, interpretation of data, drafting the article, and final approval of the submission.

All authors have reviewed this report for accuracy and have approved it for submission.

Submissions and presentations of this work:

Portions of this work have been presented at the 62 and 63rd Annual Meetings of the Society for Reproductive Investigation (2014–2015) and the 48th Annual Meeting Society for the Study of Reproduction (2015). This manuscript has not been submitted for publication to any other source.

Conflicts of Interest: We have no conflicts of interest to report and all authors have reviewed the manuscript for submission.

1. Introduction

During pregnancy, the uterus increases in size to accommodate the growing fetus, placenta, and amniotic fluid. Despite the associated increases in intra-uterine pressure, the normal myometrium adapts to prevent increased tension and remain in a quiescent state until term (Sivarajasingam et al., 2016; Sokolowski et al., 2010). Abnormal distension has been associated with early birth in twin (Gardner et al., 1995; Mercer et al., 1996), as well as approximately 10% of singleton (Lockwood and Kuczynski, 2001) preterm deliveries. Increasing uterine volume via a balloon catheter initiates prostaglandin secretion, myometrial contractions, and labor in women (Delaney et al., 2010; Manabe et al., 1984), and this process appears to occur independently of fetal signals (Yoshida and Manabe, 1988). These data suggest failure of the uterine myometrium to adapt to the continued expansion required during pregnancy may increase the risk of preterm birth (Waldorf et al., 2015).

In various animal models of uterine strain, changes in expression of chemokine, oxytocin receptor, connexin-43, and matrix metalloproteinases genes have been reported (Hua et al., 2012; Lee et al., 2015; Nguyen et al., 2016; Parry and Bathgate, 2000; Shynlova et al., 2013; Waldorf et al., 2015; Yulia et al., 2016). Fewer data are available regarding signal transduction pathways activated by uterine stress, but ERK1/2 pathway activation is a well-established strain response in pregnant myometrial cells and tissue (Li et al., 2009). In isolated rat myocytes biaxial strain is followed by phosphorylation of the kinases ERK1/2, JNK, and p38 (Oldenhof et al., 2002). Over all, protein phosphorylation is critically important for cell signaling response pathways and mediates many important functions such as protein interactions, localization, and activity (Sharma et al., 2014). *In vitro* work suggests MAPK pathways activate transcription factors such as c-fos, resulting in increased expression of contractile associated proteins to drive the onset of labor (Oldenhof et al., 2002).

We hypothesized specific phosphorylation signaling events related to the strain-induced integrin response would be upregulated in a telomerized cell culture model of human uterine smooth muscle cells. To test this hypothesis, we performed mechanical strain experiments on immortalized human uterine smooth muscle cells followed by phospho-peptide enrichment, identification, and quantitation.

2. Materials and Methods

2.1 Cell culture

Previously our lab developed telomerized pregnant human uterine smooth muscle cells (PHUSMC-hTRT) as a model of pregnant myometrium; in brief, cells were grown through passage 5 in primary culture and combined in equal numbers from three 24–29 year old Caucasian donors at full term and telomerized as described in (Heyman et al., 2013). These PHUSMC-hTRT were used at passage 27 and plated on collagen coated BioFlex® plates (Flexcell® INC, Burlington, NC) and grown in HyClone™ Dulbecco's Modified Eagle Medium (DMEM; Thermo Scientific, Pittsburg, PA) supplemented with 0.11 mg/mL Sodium Pyruvate, 10% Fetal Bovine Serum (FBS, Atlanta Biologicals, Flowery Branch,

GA), 100 U/mL penicillin 100 μg/mL streptomycin (Pen/Strep; Thermo Scientific, Pittsburgh, PA), 636 nM progesterone (P4), and 55 nM estradiol (E4). Media was refreshed every 3 days and cells were grown to confluence. At confluence, cells were placed in DMEM supplemented with 0.1% Insulin-Transferrin-Selenium-Ethanolamine (ITS-X) supplement (Thermo Scientific, Pittsburgh, PA) in the absence of FBS for 7 days to allow for growth arrest and differentiation.

2.2 Strain Experiment

Growth-arrested PHUSMC-hTRT on BioFlex® collagen plates were subjected to 18% biaxial strain for 5 min on a Flexcell® FX-5000 tension system (Flexcell® INC, Burlington, NC). PHUSMC-HTRT cells grown on BioFlex® plates not subjected to mechanical strain served as controls. Cells were lysed in 300 μL/well MAPK buffer (60 mM Tris-HCl [pH 6.8], 2 % SDS, 10% glycerol, 0.1 mM EGTA) (Singer et al., 2003) supplemented with Halt protease and phosphatase inhibitor cocktail (Thermo Scientific, Pittsburgh, PA). Strained and unstrained samples were grown on 6 well plates and randomly divided into triplicates. Lysates were probe sonicated (Qsonica, Newtown, CT) and centrifuged at 4,000 × g for 15 min. Pellets were re-suspended in MAPK buffer, precipitated in 4x volume of 100% acetone and washed three times in 4x volume of 70% acetone. Precipitates were re-suspended in 8M urea/50mM Tris-HCI (pH 8), reduced in 5 mM DTT at 37°C for 20 min in the dark, and alkylated in 10mM iodoacetamide (BioRad, Hercules, Ca) for 20 min in the dark. Samples were re-precipitated with acetone as described above and re-suspended, using sonication, in 50 mM ammonium bicarbonate. Protein samples were digested with Trypsin/Lys C mix (Promega, Madison, WI) at a 75:1 protein:protease mix overnight at 37°C, acidified in 0.1% formic acid, and desalted using Sep-Pak C18 cartridges (Waters, Milford, MA).

2.3 Phospho-peptide enrichment and LC-MS^2

Samples were enriched on IMAC columns containing nickel-nitrilotriacetic acid (Ni-NTA) agarose beads charged with TO_2 and labeled with 6-plex tandem mass (TMT) (Thermo Scientific, Pittsburgh, PA) according to the manufacturer protocols. Samples were pooled and then separated by hydrophilic interaction liquid chromatography fractionation as described previously (Albuquerque et al., 2008) for 60 min with a gradient change in solvent A (900 mL ACN + 100 mL ddH2O + 500 μL 10% TFA) from 0% solvent B (1 L ddH2O +500 μL 10% TFA) to 90% at 45 min. 40 fractions were re-suspended in 100 μL 5% acetonitrile 0.1% formic acid for mass spectrometry analysis.

Samples were analyzed using liquid chromatography tandem mass spectrometry (LC-MS^2) at the Mick Hitchcock, Ph.D. Nevada Proteomics Center (University of Nevada, Reno). Peptides were separated and analyzed using a Michrom Paradigm Multi-Dimensional Liquid Chromatography instrument (Michrom Bioresources Inc., Auburn, CA) coupled with a Thermo LTQ Orbitrap XL mass spectrometer (Thermo Fisher Scientific, San Jose, CA). Samples were dissolved in 100 μL of 0.1 % formic acid were loaded onto an Acclaim Pepmap 100 C18 LC column (100μm × 2 cm, C18 5μm, 100 Å, Thermo Fisher Scientific, San Jose, CA), eluted, and then separated by reverse phase New Objective (New Objective Inc, Woburn, MA) ReproSil-Pur C18-AQ column (3 μm, 120Å, 0.075 × 105 mm) with a gradient elution using solvent A (0.1% formic acid) and solvent B (0.1% formic acid in

acetonitrile) at a flow rate of 300 nL/min. The gradient was set from 5 % to 40 % solvent B for 90 min, increased to 80% solvent B in 10 s and held at 80% solvent B for 1 min. MS spectra were recorded over the mass range of m/z 400–1600 with resolution of 60,000. The three most intense ions were isolated for fragmentation in the linear ion trap using collision induced dissociation (CID) with minimal signal of 500% and collision energy of 35.0% using higher-energy collision dissociation (HCD) with minimal signal of 1000%, Collision energy of 55.0%, and an activation time of 30 ms. Dynamic exclusion was implemented with 2 repeat counts, repeat duration of 15 s, and exclusion duration of 90 s. The mass spectrometry proteomics data have been deposited to the ProteomeXchange Consortium (Dennis et al., 2012) via the PRIDE partner repository with the dataset identifier PXD002538 and 10.6019/PXD002538.

2.4 Peptide and Protein Identification

Scaffold (version 4.4.1.1, Proteome Software Inc., Portland, OR) was used to validate MS/MS based peptide and protein identifications. Identification and quantification of peptides was achieved by combining CID and HCD fragmentation. CID fragmentation energy was fine tuned to avoid dissociation of phosphorylation groups. This reduced collision energy results in loss of approximately 30% of ions in the lower weight register. To maintain a high confidence of peptide identification and a valuable TMT labeled quantification signal, the top three peptides selected during the first mass spectrometry analysis were subjected to HCD. HCD spectra were used for quantification and integrated with the identifications obtained from CID spectra with a confidence threshold of 90%. All MS/MS samples were analyzed using SEQUEST (Thermo Fisher Scientific, San Jose, CA, USA; version 1.0). SEQUEST was set up to search the ipi.HUMAN_decoy.v3.87 database, (Version 3.87, 182928 entries) assuming the digestion enzyme strict Trypsin/Lys-C.

2.5 Bioinformatics

Sample sizes were chosen as n=3 in both cohorts, where each sample replicate was a randomly chosen combination of 72 unique cell-lysis aliquots. As we were expecting effect sizes between cohorts to be large (Cohen, 1988), we estimated that sample sizes with n=3 would be sufficient. This is a novel experiment with no preliminary data to use as a pilot power study.

Upon generating the data, we did perform standard power studies on the 74 proteins/peptides that showed the greatest statistical significance upon hypothesis testing. Of these 74 proteins, the power of the hypothesis test in 60 (81%) reached a power of 80% or greater (80% to 99.99%), with a significance level of alpha=.05. The power of the remaining 14 proteins ranged from 73.3% to 79.1%.

The final data set was log-transformed to follow a normal distribution, and a simple t-test was performed to test for differences in the means across the two cohorts on all peptides that contained the same post translational modification (PTM) configuration. A multiple testing correction (Benjamini and Hochberg, 1995) was performed to adjust for the false discovery rate.

2.6 Gene Ontology analysis

The functional categories of all differentially regulated phospho-proteins were classified by the Panther Gene Ontology (GO) algorithm (http://www.pantherdb.org/).

2.6 Ingenuity pathway analysis (IPA)

Mechano-transduction induced phosphorylation networks were analyzed using Ingenuity Pathway Analysis software (IPA) (Qiagen, Redwood City, CA). Annotated phospho-proteins were included in the IPA searches based on a cut off of 1.5-fold change and p-value < 0.05. Each protein symbol was mapped to its corresponding gene and set within the context of its associated partners based on the Ingenuity Pathways Knowledge Base (IPKD).

The significance of the association between the data set and the canonical pathway was determined based on two parameters: (1) A ratio of the number of genes from the data set that map to the pathway divided by the total number of genes that map to the canonical pathway and (2) a *P* value calculated using Fischer's exact test determining the probability that the association between the genes in the data set and the canonical pathway is due to chance alone.

2.8 Western Blot Analysis

Growth arrested PHUSMC-HTRT cells on BioFlex® collagen plates were subjected to 18% biaxial strain for 5 min on a Flexcell® FX-5000 tension system (Flexcell® INC, Burlington, NC). PHUSMC-HTRT cells grown on BioFlex® plates not subjected to strain served as controls. Lysates were bath sonicated for 10 minutes and centrifuged at 13,000 × g for 15 min.

Samples were electrophoresed on sodium dodecyl sulfate 4% to 20% gradient polyacrylamide gels and western blotted according to manufacturer instructions (BioRad, Hercules, Ca) with the following primary antibodies: p38 MAPK (D13E1) XP® #8690; Phospho-p38 (Thr180/Tyr182) (D3F9) XP® #4511; HSP27 Antibody Sampler Kit #12594 were from Cell Signaling Technology (Beverly, MA); Primary antibodies were detected with IRDye 680LT goat anti-rabbit (LiCor Biosciences, Lincoln, NE) or IRDye 800LT donkey anti-mouse (827-08364, Rockland Immunochemicals, Gilbertsville, PA). Band intensities were quantified with an Odyssey Infrared Imaging System (LiCor Biosciences). Phosphoprotein band intensities were normalized to total protein expression. Normalized group values were compared on Prism version 6 (GraphPad) with a one-way ANOVA.

3. Results

3.1 Peptide Identifications

We utilized mass spectrometry to reveal the phospho-proteomic changes initiated by acute 18% biaxial mechanical strain for 5 min (Fig 1) in PHUSMC-hTRTs compared to non-strained controls. We identified 1176 phospho-sites on 1098 phospho-peptides at a 1% false discovery rate and a 90% protein confidence threshold. These phosphorylation events were comprised of 849 serine (72.2%), 264 threonine (22.4%), and 63 tyrosine (5.2%). These numbers are similar to those found in mouse tissue and HeLa cells (Huttlin et al., 2010;

Zarei et al., 2011). Quantitation and statistical analysis revealed a greater than a 1.5 fold change at 204 unique protein phosphorylation sites. Increases in phosphorylation were seen at 141 phospho-sites, while decreases in phosphorylation were seen at 63 phospho-sites.

3.2 Gene Ontology

Proteins containing differentially phosphorylated sites were annotated, to basic cellular processes, by Panther online software (Thomas et al., 2003) into 12 functional categories. The largest category was extracellular signaling transduction (25.2%) which is broken down into 7 sub-categories including extracellular matrix protein (6%), transporter (5%), transmembrane receptor regulatory/adaptor protein (1%), cell adhesion molecule (5%), membrane traffic protein (1%), cell junction protein (2%), and receptor proteins (5%) (Fig 2). The second and third most abundant categories were nucleic acid binding (15.7%) and transcription factors respectively (13.3%).

3.3 Ingenuity Pathway Analysis

Phosphorylation changes were mapped to 220 total pathways, based on a 1.5 fold-change with a p-value of < 0.05, of which the top 25 were considered for further analysis (Fig 3). IPA network analysis revealed that 10 of these pathways collectively grouped into a functional network of 13 proteins (Fig 4). IPA then combined these proteins together to reveal an interconnected set of phospho-protein interactions (Fig 5). Within this interaction network, we observed the specific phosphorylation of previously annotated sites of activation ERK1/2 at T183 and Y185, and heat shock protein beta-1 (HSPB1) at S82. In addition, we detected increased phosphorylation of MYL9 at sites T19 and S20. These patterns are consistent with the idea that contractile mechanisms are upregulated in response to strain activation.

3.4 Western Blot analysis

Confirmation of mass spectrometry analysis by western blot showed increased phosphorylation of key proteins p38, ERK1/2 and HSPB1, at previously annotated sites after 5 min of 18% biaxial mechanical strain (Fig 6).

4. Discussion

Our phospho-proteomic snapshot revealed the activation of both focal adhesion-associated and novel strain-responsive signaling pathways in human myometrial cells. We found differential phosphorylation of ERK1/2, vinculin, heat shock protein B1 (HSPB1), protein kinase C (PKCα) and p21 activated kinase 2 (PAK2) which IPA revealed to be associated with the downstream activity of the integrin linked kinase pathway. In agreement with previous tissue experiments (Yunping Li et al., 2009), we found increased ERK1/2 phosphorylation levels at T185 after 5 min of strain in myometrial cells. This site is one of two key regulatory sites of ERK 2 phosphorylation (Ahn et al., 1991; Anderson et al., 1990; Boulton et al., 1991). Myometrial strain has previously been shown to activate focal adhesion and ERK/MAP kinase signaling pathways (Macphee and Lye, 2000; Oldenhof et al., 2002; Sooranna et al., 2005; Wu et al., 2008). These data, combined with our results and the observation that the ERK inhibitor U-0126 delays preterm labor in rats treated with

RU-486 (Li et al., 2004), suggest a major role for ERK activation in the regulation of gestational timing.

HSPB1 is a small 27 kD heat shock protein that has been implicated in a wide variety of cellular functions including protection from heat stress, actin remodeling, and regulation of smooth muscle contraction. Cell contractility in smooth muscle cells has been linked to phosphorylation of HSPB1 on S82 (Gerthoffer and Gunst, 2001) which also has been linked to ERK activity (Robitaille et al., 2010). HSPB1 phosphorylation is also regulated by p38 kinase in response to cyclic strain in cultured fibroblasts and contributes to actin remodeling (Hoffman et al., 2017). Additionally, many of the functional roles of HSPB1 are regulated by PTMs, particularly the phosphorylation of two sites (S15, S82) (Rouse et al., 1994). These data suggest HSPB1 may be a key regulator of contractile phenotype and play a significant role in the induction of labor.

Phosphorylation of PAK2 and HSPB1 (at site S82) were increased in response to strain and suggest a mechanistic link between the mechanical strain response and the development of a contractile phenotype. PAK2 has been shown to down regulate cofilin via phosphorylation (Kosoff et al., 2015) and PKC inhibition reduces HSPB1 S82 phosphorylation levels in vascular smooth muscle (Moreno-Domínguez et al., 2014). Since cofilin phosphorylation reduces actin polymerization, while HSPB1 enhances polymerization, the cofilin and HSPB1 S82 phosphorylation states are important regulators of smooth muscle actin polymerization and may regulate strain induced contractility.

While we found direct evidence of HSPB1 and p38 activation, we did not find phosphorylation sites on PKCα and PAK2 that correlate to previously annotated sites. It is possible that the phosphorylation sites we identified represent alternative activation sites related to a particular temporal or physical pattern of cellular activity. The significance of this phosphorylation pattern needs to be further investigated. IPA results suggest a central role for vimentin in the response to acute mechanical strain. ERK1/2 and HSPB1 regulate cytoskeletal remodeling through interaction with vimentin, an intermediate filament protein that is important to cellular tensile strength particularly in the cytoplasm (Guo et al., 2013). We saw increased phosphorylation of a number of amino acids on vimentin fibers in response to mechanical strain. Phosphorylation of vimentin at S56 is PAK1 dependent in airways smooth muscle cells responding to contractile stimulation (Tang and Gerlach, 2017); however, vimentin is regulated by a variety of kinases and phosphatases (Eriksson et al., 2004) and the long-term downstream, temporal, and mechanical consequences of such phosphorylation patterns may be related to HSPB1 and PAK2 phosphorylation via mechanical activation.

Smooth muscle contraction is regulated by the kinase/phosphatase activities of myosin light chain kinase (MLCK) and myosin light chain phosphatase (MYPT1) (Aguilar and Mitchell, 2010). Phosphorylation of MLCK and activation of the serine/threonine kinases are responsible for down regulating phosphorylation of MYPT1 leading to increased calcium sensitivity (Amano et al., 1996; Kimura et al., 1996). Focal adhesions are known activators of MLCK phosphorylation and of myosin light chain 9 (MYL9) which increases calcium sensitivity and force of contraction (Wray, 1993). We detected phosphorylation of MYL9 at

sites T19 and S20 demonstrating that contractile mechanisms were engaged subsequent to strain activation. In addition, protein kinase C is known to phosphorylate CPI-17 leading to the phosphorylation dependent deactivation of MYPT1 and increased calcium sensitivity (Somlyo and Somlyo, 2003). The implication of the observed phosphorylation patterns suggests increased calcium sensitivity is induced by strain activation. A proposed schematic of strain induced calcium sensitization based on our data is shown (Fig 7).

In addition to previously annotated phosphorylation sites, we discovered proteins such as PAK2, DOCK1, PPP1R12A, and PTPN11, which were phosphorylated on unannotated sites; however, pathway signaling analysis by IPA predicts that they are activated, either by temporal separation of the signal or a novel activation from unannotated phospho-sites. The annotation of these phosphorylation sites and the temporal separation of such events still needs to be investigated.

Cultured cell models provide a valuable tool to obtain insight into the regulation of myometrial function (Mosher et al., 2013) and have the advantage of allowing analysis of the effect of mechanical strain on signal transduction events specifically in myometrial cells in the absence of complicating factors such as maternal age, race, gestational age, fetal sex, and variations in the *in vivo* hormone environment (Burris and Collins, 2010; Challis et al., 2013; Myatt et al., 2012). However, cultured cells are isolated from the influence of other cell types present in the parent tissue and the two-dimensional environment may not approximate 3D tissue structures (Smith et al., 2017; Souza et al., 2017; Zhang et al., 2013). Cultured, non-laboring human myometrial cells undergo gene expression changes indicative of a contractile, laboring phenotype (Ilicic et al., 2017), although it is not clear if these changes correspond to protein level and phenotypic changes. While it is not currently possible to mimic the mechanical forces that confront the uterus during pregnancy precisely, 5 min of isolated mechanical strain provides insight into the proteins and pathways that contribute to the initiation of cellular responses. As such, this work provides a starting point for elucidation of the interaction of molecular pathways activated by mechanical strain, future work is needed to confirm these data in tissue or animal models.

Acknowledgments

Jonathon James for graphic design, Janet A. Lambert for detailed review, and Patrick Barnett for Python script development. This work was supported by the Mountain West Clinical Translational Research-Infrastructure Network under a grant from the National Institute of General Medical Sciences (NIH award number 1U54GM104944), Nevada INBRE which is funded by grants from the National Institute of General Medical Sciences (8 P20 GM103440) from the National Institutes of Health, and a Pathway to Independence Award from the Eunice Kennedy Shriver National Institute of Child Health and Human Development (NIH award number R00HD067342) to Heather Burkin. The content is solely the responsibility of the authors and does not necessarily represent the official views of the National Institute of Health.

References

Aguilar HN, Mitchell BF. Physiological pathways and molecular mechanisms regulating uterine contractility. Hum Reprod Update. 2010; 16:725–744. [PubMed: 20551073]

Ahn NG, Seger R, Bratlien RL, Diltz CD, Tonks NK, Krebs EG. Multiple components in an epidermal growth factor-stimulated protein kinase cascade. J Biol Chem. 1991; 266:4220–4227. [PubMed: 1705548]

Albuquerque CP, Smolka MB, Payne SH, Bafna V, Eng J, Zhou H. A multidimensional chromatography technology for in-depth phosphoproteome analysis. Mol Cell Proteomics. 2008; 7:1389–1396. [PubMed: 18407956]

Amano M, Ito M, Fukata Y, Chihara K, Nakano T, Matsuura Y, Kaibuchi K. Phosphorylation and Activation of Myosin by Rho-associated Kinase (Rho Kinase). J Biol Chem. 1996; 271:20246–20249. [PubMed: 8702756]

Anderson NG, Maller JL, Tonks NK, Sturgill TW. Requirement for integration of signals from two distinct phosphorylation pathways for activation of MAP kinase. Nature. 1990; 343:651–653. [PubMed: 2154696]

Benjamini Y, Hochberg Y, Benjamini Y, Hochberg Y. Controlling the false discovery rate: a practical and powerful approach to multiple testing. J R Stat Soc B. 1995; 57:289–300.

Boulton TG, Nye SH, Robbins DJ, Ip NY, Radzlejewska E, Morgenbesser SD, DePinho RA, Panayotatos N, Cobb MH, Yancopoulos GD. ERKs: A family of protein-serine/threonine kinases that are activated and tyrosine phosphorylated in response to insulin and NGF. Cell. 1991; 65:663–675. [PubMed: 2032290]

Burris HH, Collins JW. Race and preterm birth--the case for epigenetic inquiry. Ethn Dis. 2010; 20:296–299. [PubMed: 20828105]

Challis J, Newnham J, Petraglia F, Yeganegi M, Bocking A. Fetal sex and preterm birth. Placenta. 2013; 34:95–99. [PubMed: 23261268]

Cohen, J. Statistical power analysis for the behavioral sciences. Lawrence Erlbaum Associates; Mahwah: 1988. p. 567

Delaney S, Shaffer BL, Cheng YW, Vargas J, Sparks TN, Paul K, Caughey AB. Labor induction with a Foley balloon inflated to 30 mL compared with 60 mL: a randomized controlled trial. Obstet Gynecol. 2010; 115:1239–45. [PubMed: 20502296]

Dennis MK, Field AS, Burai R, Ramesh C, Whitney K, Bologa CG, Oprea TI, Yamaguchi Y, Hayashi S, Sklar La, Hathaway HJ, Arterburn JB, Prossnitz ER. ProteomeXchange provides globally co-ordinated proteomics data submission and dissemination. Nat Biotechnol. 2012; 127:358–366.

Eriksson JE, He T, Trejo-Skalli AV, Härmälä-Braskén AS, Hellman J, Chou YH, Goldman RD. Specific in vivo phosphorylation sites determine the assembly dynamics of vimentin intermediate filaments. J Cell Sci. 2004; 117:919–932. [PubMed: 14762106]

Gardner MO, Goldenberg RL, Cliver SP, Tucker JM, Nelson KG, Copper RL. The origin and outcome of preterm twin pregnancies. Obstet Gynecol. 1995; 85:553–557. [PubMed: 7898832]

Gerthoffer WT, Gunst SJ. Invited review: focal adhesion and small heat shock proteins in the regulation of actin remodeling and contractility in smooth muscle. J Appl Physiol. 2001; 91:963–972. [PubMed: 11457815]

Guo M, Ehrlicher AJ, Mahammad S, Fabich H, Jensen MH, Moore JR, Fredberg JJ, Goldman RD, Weitz Da. The role of vimentin intermediate filaments in cortical and cytoplasmic mechanics. Biophys J. 2013; 105:1562–1568. [PubMed: 24094397]

Heyman NS, Cowles CL, Barnett SD, Wu YY, Cullison C, Singer CA, Leblanc N, Buxton ILO. TREK-1 currents in smooth muscle cells from pregnant human myometrium. AJP Cell Physiol. 2013; 305:C632–C642.

Hoffman L, Jensen CC, Yoshigi M, Beckerle M. Mechanical signals activate p38 MAPK pathway-dependent reinforcement of actin via mechanosensitive HspB1. Mol Biol Cell. 2017; 28:2661–2675. [PubMed: 28768826]

Hua R, Pease JE, Sooranna SR, Viney JM, Nelson SM, Myatt L, Bennett PR, Johnson MR. Stretch and inflammatory cytokines drive myometrial chemokine expression via NF-κB activation. Endocrinology. 2012; 153:481–491. [PubMed: 22045664]

Huttlin EL, Jedrychowski MP, Elias JE, Goswami T, Rad R, Beausoleil Sa, Villén J, Haas W, Sowa ME, Gygi SP. A tissue-specific atlas of mouse protein phosphorylation and expression. Cell. 2010; 143:1174–1189. [PubMed: 21183079]

Ilicic M, Butler T, Zakar T, Paul JW. The expression of genes involved in myometrial contractility changes during ex situ culture of pregnant human uterine smooth muscle tissue. J Smooth Muscle Res. 2017; 53:73–89. [PubMed: 28652518]

Kimura K, Ito M, Amano M, Chihara K, Fukata Y, Nakafuku M, Yamamori B, Feng J, Nakano T, Okawa K, Iwamatsu a, Kaibuchi K. Regulation of myosin phosphatase by Rho and Rho-associated kinase (Rho-kinase). Science. 1996; 273:245–248. [PubMed: 8662509]

Kosoff RE, Aslan JE, Kostyak JC, Dulaimi E, Chow HY, Prudnikova TY, Radu M, Kunapuli SP, Mccarty OJT, Chernoff J. Pak2 restrains endomitosis during megakaryopoiesis and alters cytoskeleton organization. Blood. 2015; 125:2995–3006. [PubMed: 25824689]

Lee YH, Shynlova O, Lye SJ. Stretch-induced human myometrial cytokines enhance immune cell recruitment via endothelial activation. Cell Mol Immunol. 2015; 12:231–42. [PubMed: 24882387]

Li Y, Je HD, Malek S, Morgan KG. Role of ERK1/2 in uterine contractility and preterm labor in rats. Am J Physiol Regul Integr Comp Physiol. 2004; 287:R328–R335. [PubMed: 15072963]

Li Y, Reznichenko M, Tribe RM, Hess PE, Taggart M, Kim H, DeGnore JP, Gangopadhyay S, Morgan KG. Stretch activates human myometrium via ERK, caldesmon and focal adhesion signaling. PLoS One. 2009; 4:e7489. [PubMed: 19834610]

Li Y, Reznichenko M, Tribe RM, Hess PE, Taggart M, Kim HR, DeGnore JP, Gangopadhyay S, Morgan KG. Stretch activates human myometrium via ERK, caldesmon and focal adhesion signaling. PLoS One. 2009; 4:e7489. [PubMed: 19834610]

Lockwood CJ, Kuczynski E. Risk stratification and pathological mechanisms in preterm delivery. Paediatr Perinat Epidemiol. 2001; 15(Suppl 2):78–89. [PubMed: 11520402]

Macphee DJ, Lye SJ. Focal adhesion signaling in the rat myometrium is abruptly terminated with the onset of labor. Endocrinology. 2000; 141:274–283. [PubMed: 10614648]

Manabe Y, Mori T, Yoshida Y. Decidual morphology and F prostaglandin in amniotic fluid in stretch-induced abortion. Obstet Gynecol. 1984; 64:661–665. [PubMed: 6493658]

Mercer BM, Goldenberg RL, Das A, Moawad AH, Iams JD, Meis PJ, Copper RL, Johnson F, Thom E, McNeills D, Miodovnik M, Menard MK, Caritis SN, Thurnau GR, Bottoms SF, Roberts J. The preterm prediction study: a clinical risk assessment system. Am J Obstet Gynecol. 1996; 174:1885. [PubMed: 8678155]

Moreno-Domínguez A, El-Yazbi AF, Zhu HL, Colinas O, Zhong XZ, Walsh EJ, Cole DM, Kargacin GJ, Walsh MP, Cole WC. Cytoskeletal reorganization evoked by Rho-associated kinase- and protein kinase C-catalyzed phosphorylation of cofilin and heat shock protein 27, respectively, contributes to myogenic constriction of rat cerebral arteries. J Biol Chem. 2014; 289:20939–20952. [PubMed: 24914207]

Mosher AA, Rainey KJ, Bolstad SS, Lye SJ, Mitchell BF, Olson DM, Wood SL, Slater DM. Development and validation of primary human myometrial cell culture models to study pregnancy and labour. BMC Pregnancy Childbirth. 2013; 13:1–14. [PubMed: 23324161]

Myatt L, Eschenbach DA, Lye SJ, Mesiano S, Murtha AP, Williams SM, Pennell CE. A standardized template for clinical studies in preterm birth. Reprod Sci. 2012; 19:474–82. [PubMed: 22344727]

Nguyen TTTN, Shynlova O, Lye SJ. Matrix Metalloproteinase Expression in the Rat Myometrium During Pregnancy, Term Labor, and Postpartum. Biol Reprod. 2016; 95:1–14. [PubMed: 27387869]

Oldenhof A, Shynlova O, Liu M, Langille B, Lye S. Mitogen-activated protein kinases medial stretch-induced c-fos mRNA expression in myometrial smooth muscle cells. Am J Physiol Cell Physiol. 2002; 283:C1530–C1539. [PubMed: 12372814]

Parry LJ, Bathgate RA. The role of oxytocin and regulation of uterine oxytocin receptors in pregnant marsupials. Exp Physiol. 2000; 85:91S–99S. [PubMed: 10795911]

Robitaille H, Simard-Bisson C, Larouche D, Tanguay RM, Blouin R, Germain L. The small heat-shock protein Hsp27 undergoes ERK-dependent phosphorylation and redistribution to the cytoskeleton in response to dual leucine zipper-bearing kinase expression. J Invest Dermatol. 2010; 130:74–85. [PubMed: 19675578]

Rouse J, Cohen P, Trigon S, Morange M, Alonso-Llamazares A, Zamanillo D, Hunt T, Nebreda AR. A novel kinase cascade triggered by stress and heat shock that stimulates MAPKAP kinase-2 and phosphorylation of the small heat shock proteins. Cell. 1994; 78:1027–1037. [PubMed: 7923353]

Sharma K, D'Souza RCJ, Tyanova S, Schaab C, Wiśniewski JR, Cox J, Mann M. Ultradeep Human Phosphoproteome Reveals a Distinct Regulatory Nature of Tyr and Ser/Thr-Based Signaling. Cell Rep. 2014; 8:1583–1594. [PubMed: 25159151]

Shynlova O, Lee YH, Srikhajon K, Lye SJ. Physiologic uterine inflammation and labor onset: integration of endocrine and mechanical signals. Reprod Sci. 2013; 20:154–167. [PubMed: 22614625]

Singer, Ca, Baker, KJ., McCaffrey, A., AuCoin, DP., Dechert, Ma, Gerthoffer, WT. p38 MAPK and NF-kappaB mediate COX-2 expression in human airway myocytes. Am J Physiol Lung Cell Mol Physiol. 2003; 285:L1087–L1098. [PubMed: 12871860]

Sivarajasingam SP, Imami N, Johnson MR. Myometrial cytokines and their role in the onset of labour. J Endocrinol. 2016; 231:R101–R119. [PubMed: 27647860]

Smith I, Silveirinha V, Stein JL, De Torre-ubieta L, Farrimond JA, Williamson EM, Whalley BJ. Human neural stem cell-derived cultures in three- dimensional substrates form spontaneously functional neuronal networks. J Tissue Eng Regen Med. 2017; 11:1022–1033. [PubMed: 25712225]

Sokolowski P, Saison F, Giles W, McGrath S, Smith D, Smith J, Smith R. Human uterine wall tension trajectories and the onset of parturition. PLoS One. 2010; 5:e11037. [PubMed: 20585649]

Somlyo AP, Somlyo AV. Ca2+ sensitivity of smooth muscle and nonmuscle myosin II: modulated by G proteins, kinases, and myosin phosphatase. Physiol Rev. 2003; 83:1325–1358. [PubMed: 14506307]

Sooranna SR, Engineer N, Loudon JAZ, Terzidou V, Bennett PR, Johnson MR. The mitogen-activated protein kinase dependent expression of prostaglandin H synthase-2 and interleukin-8 messenger ribonucleic acid by myometrial cells: The differential effect of stretch and interleukin-1β. J Clin Endocrinol Metab. 2005; 90:3517–3527. [PubMed: 15784717]

Souza GR, Tseng H, Gage JA, Mani A, Desai P, Leonard F, Liao A, Longo M, Refuerzo JS, Godin B. Magnetically bioprinted human myometrial 3D cell rings as a model for uterine contractility. Int J Mol Sci. 2017; 18:1–10.

Tang DD, Gerlach BD. The roles and regulation of the actin cytoskeleton, intermediate filaments and microtubules in smooth muscle cell migration. Respir Res. 2017; 18:1–12. [PubMed: 28049526]

Thomas PD, Campbell MJ, Kejariwal A, Mi H, Karlak B. PANTHER: A Library of Protein Families and Subfamilies Indexed by Function. Genome Res. 2003; 13:2129–2141. [PubMed: 12952881]

Waldorf KMA, Singh N, Mohan AR, Young RC, Ngo L, Das A, Tsai J, Bansal A, Paolella L, Herbert BR, Sooranna SR, Gough GM, Astley C, Vogel K, Baldessari AE, Bammler TK, MacDonald J, Gravett MG, Rajagopal L, Johnson MR. Uterine overdistention induces preterm labor mediated by inflammation: Observations in pregnant women and nonhuman primates. Am J Obstet Gynecol. 2015; 213:e1–e19.

Wray S. Uterine contraction and physiological mechanisms of modulation. Am J Physiol. 1993; 264:53–54.

Wu X, Morgan KG, Jones CJ, Tribe RM, Taggart MJ. Myometrial mechanoadaptation during pregnancy: Implications for smooth muscle plasticity and remodelling. J Cell Mol Med. 2008; 12:1360–1373. [PubMed: 18363833]

Yoshida Y, Manabe Y. Stretch-induced delivery is independent of the functional fetal role and dysfunction of the amnion and decidua: A morphologic and enzyme cytochemical study. Am J Obstet Gynecol. 1988; 159:1293–1298. [PubMed: 3189461]

Yulia A, Singh N, Lei K, Sooranna SR, Johnson MR. Cyclic AMP effectors regulate myometrial oxytocin receptor expression. Endocrinology. 2016; 157:4411–4422. [PubMed: 27673556]

Zarei M, Sprenger A, Metzger F, Gretzmeier C, Dengjel J. Comparison of ERLIC-TiO(2), HILIC-TiO(2), and SCX-TiO(2) for Global phosphoproteomics Approaches. J Proteome Res. 2011; 10:3474–3483. [PubMed: 21682340]

Zhang D, Shadrin I, Lam J, Xian HQ, Snodgrass R, Bursac N. Tissue-engineered Cardiac Patch for Advanced Functional Maturation of Human ESC-derived Cardiomyocytes. Biomaterials. 2013; 34:5813–5820. [PubMed: 23642535]

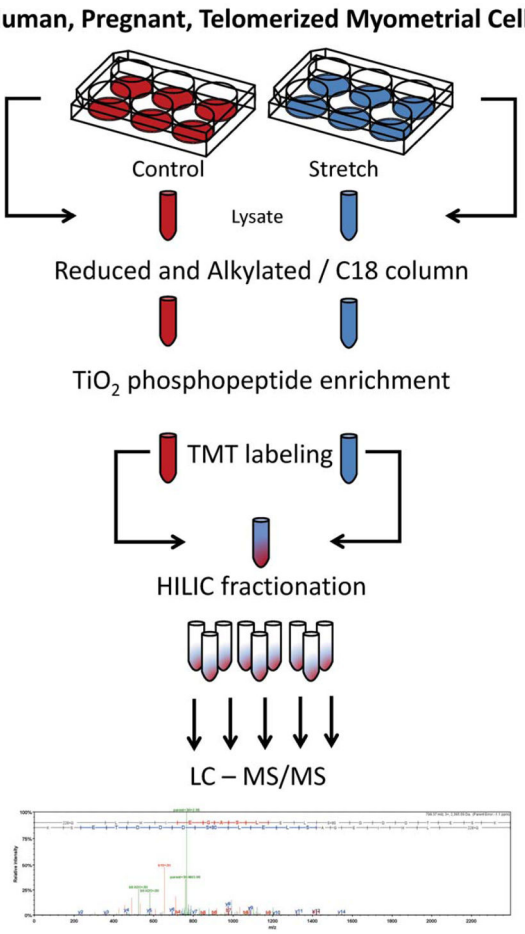

Fig. 1. Myometrial cell mechanical strain experimental design

Growth arrested PHUSMC-hTRT on BioFlex® plates were subjected to 18% biaxial mechanical strain for 5 min. Annotated SEQUEST peptide results were analyzed using IPA for pathway associations. Specific phospho-site annotations were taken from the Phosphosite.org database.

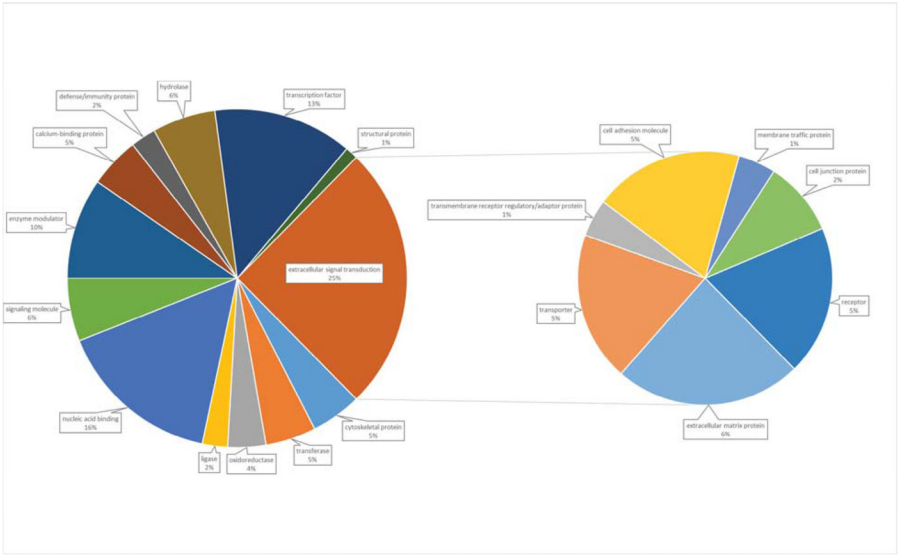

Fig. 2.

GO analysis of protein functional categories represented by differentially phosphorylated proteins after exposure to 5 minutes of mechanical stretch. Go annotations from the panther analysis data base revealed 19 categories of protein functions.

Fig. 3. Top 25 differentially regulated pathways

as determined using IPA software. Over-represented pathways were sorted by log2-fold-change (0.6) and the top 25 were selected for additional analysis. Red and green bars represent the percentage of pathway proteins either up (red) or down (green) regulated quantified on the top axis as compared to the total number of proteins annotated to each pathway shown as black numbers after each bar. The negative log of the p-value of each pathway enrichment is shown as a yellow line with quantification on the bottom axis.

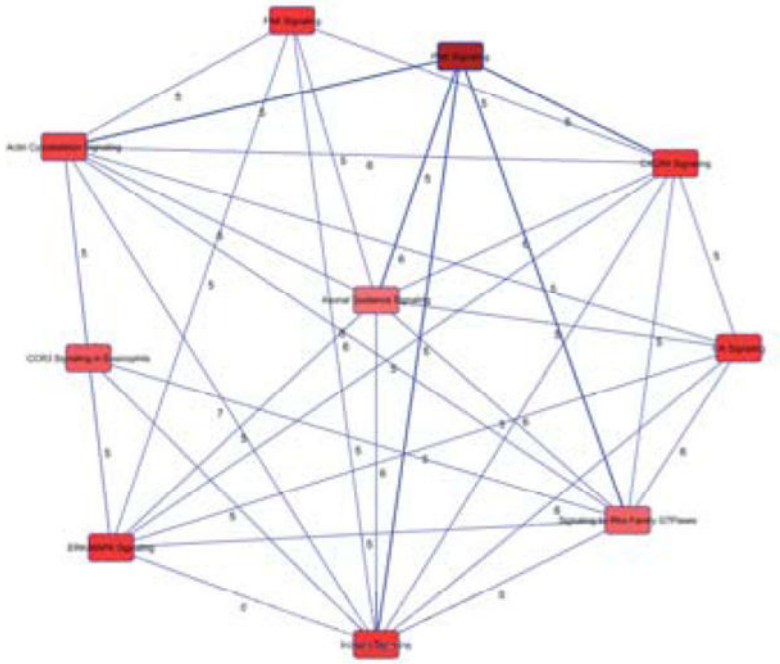

Fig. 4. Overlapping Canonical

Pathways generated by IPA. A pathway network was generated, from the top 25 over represented pathways determined by IPA, to reveal the most functionally active proteins with differential phosphorylation. Nodes represent pathways and edges are labeled with the number of common proteins connecting each node.

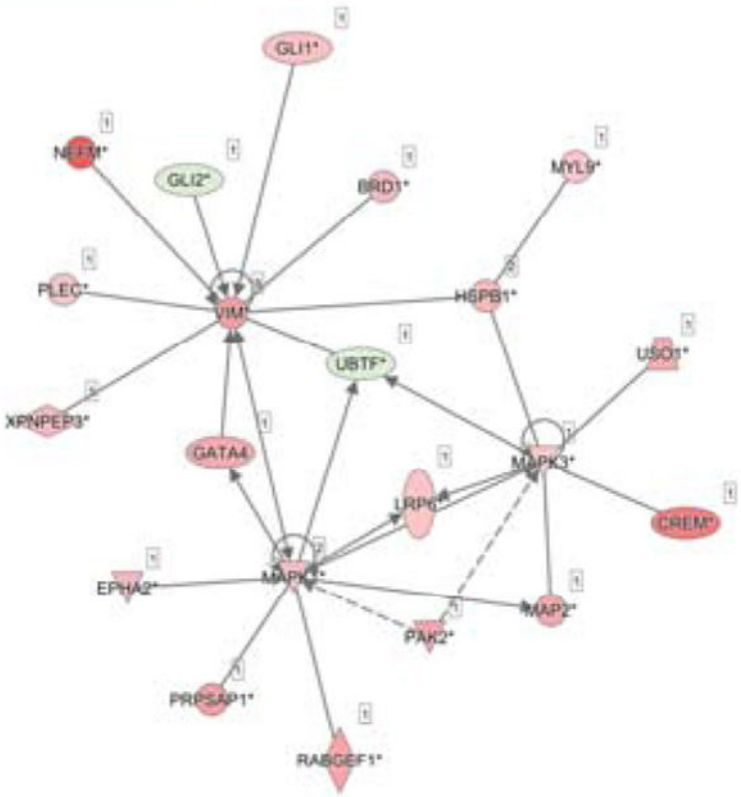

Fig. 5. Network analysis of the most functionally active proteins

represented by the edges of Fig. B. All unique proteins counted as part of all the edges were collected and networked by IPA. These proteins form the core of differentially expressed proteins at 5 min of mechanical strain. Proteins in pink had increased phosphorylation and proteins in green had decreased phosphorylation.

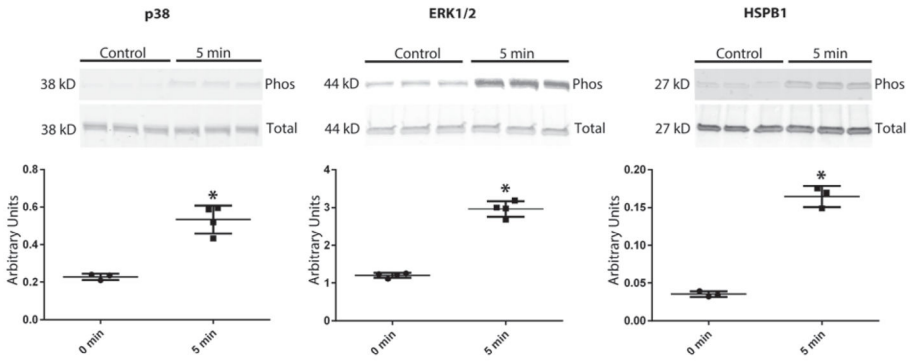

Fig. 6. Western blot validation of HSPB1 pathway activation

This tonic mechanical strain revealed phosphorylation of ERK1/2 and HSPB1. Additionally, we saw increased phosphorylation of p38 kinase, an activator of HSPB1 and a protein predicted by IPA to be activated. Statistical analysis of all blots was performed by normalization of phosphorylation to total protein with (*) representing a p value of <0.001.

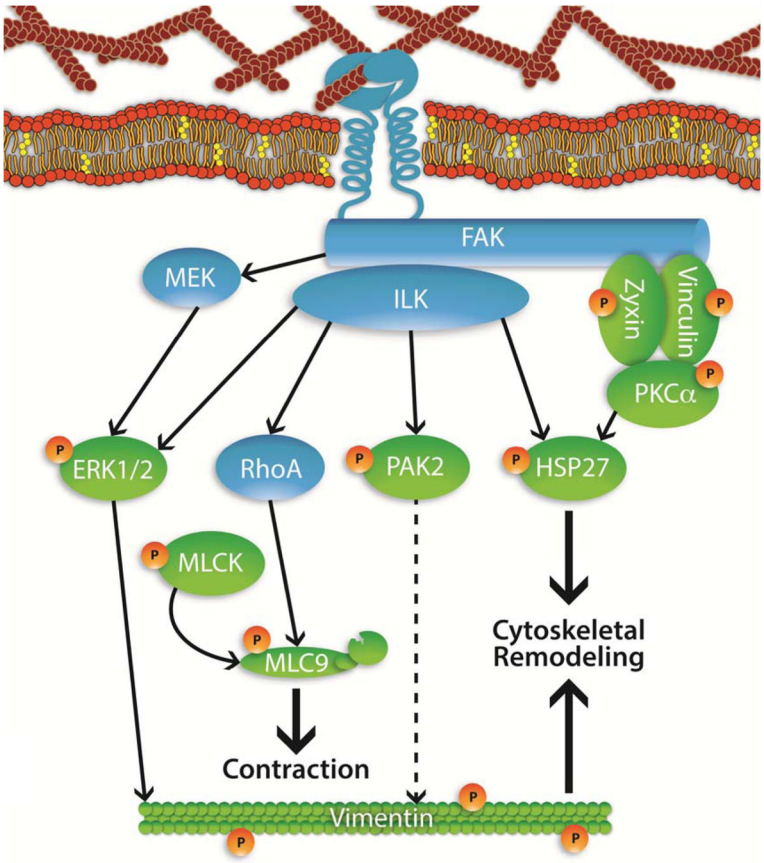

Fig. 7. Proposed mechanical strain-induced phosphorylation in myometrial cells

Experimentally determined phosphorylated proteins at 5 min (green with orange P) with pathway proteins (blue) that were not experimentally observed to be phosphorylated after 5 min of mechanical strain. Associations based on literature searches and phospho-site annotation (HSPB1 represented here as HSP27).